Supporting Information

Polarization-Encrypted Orbital Angular Momentum Multiplexed Metasurface Holography

Hongqiang Zhou,[†] Basudeb Sain,[‡] Yongtian Wang,[*,†] Christian Schlickriede,[‡] Ruizhe Zhao,[†] Xue Zhang,[†] Qunshuo Wei,[†] Xiaowei Li,[§] Lingling Huang,[*,†] Thomas Zentgraf[*,‡]

[†]School of Optics and Photonics, Beijing Institute of Technology, Beijing, 100081, China

[‡]Department of Physics, Paderborn University, Warburger Straße 100, 33098 Paderborn, Germany

[§]Laser Micro/Nano-Fabrication Laboratory, School of Mechanical Engineering, Beijing Institute of Technology, Beijing 100081, China

[*]Email: wyt@bit.edu.cn

[*]Email: huanglingling@bit.edu.cn

[*]Email: thomas.zentgraf@uni-paderborn.de

1. Modified GS Algorithm for OAM and Polarization Selective Hologram

The modified GS algorithm flow chart for multiple OAM and polarization encryption is shown in **Figure S1a**. Since we utilize a vortex array for the indicator of the incident beam in the cross-polarization channel, the φ_{xy} is calculated independently and is inserted into the iterative loop for the optimization of the other two holographic images. By using such loops, we build the quantitative relationship of $\varphi_{s3}=\left(2\varphi_{s2}-\varphi_{s1}+\pi\right)-l_3\varphi$ for the three channels. Here, the subscript ***s*** means the phase carried by the nanostructure. Note, we carefully set the vortex array with a topological charge of (−40, −20, 0, 20, 40) by referring our method proposed in Ref. 1. When the conjugate OAM illuminates, the corresponding specific vortex beam will be quenched from a donut to a bright spot. Next, we added two different topological charge numbers (l_1=40, l_3=20) to encrypt φ_{s1} and φ_{s3} in the iterative loop. After a sufficient number of iterations, two optimized holograms with a quantitative relationship for the two co-polarization channels are obtained.

To explore the optical camouflage by mimicking the STED concept, **Figure S1b** shows the generation process of a phase-only hologram (φ_{xx}) in T_{xx}. Because the two co-polarization channels are totally independent, the same generation algorithm is applied in the other channel T_{yy}. Different from the traditional GS algorithm, the multiple OAM ($l_4\varphi$ and $l_5\varphi$) is added in the process of Fourier transform (FFT) and inverse Fourier transform (IFFT). To implement the erasing/modification effect to depict the sophisticated details between two images, we combine two phases of φ_{t1} and φ_{t2} encrypted with OAM ($l_4\varphi$ and $l_5\varphi$, where l_4=0, l_5=40) for the final hologram within one polarization channel. In our experiment, the target image (T_1) is demonstrated when the incident plane wave (l=0), and the modified target image (T_2) is reconstructed when the incident beam carries l=40. The OAM here serves as an eraser to modify the information.

Note, for the better representation of the OAM holography, the target images are sampled to dot arrays before sending them to the GS iteration. The sampling interval and the size of the sampling spot are optimally selected according to the incident OAM beams. Hence, we can ensure the OAM selectivity to a specific topological charge while for other OAM modes, the reconstructed images would be blurred.

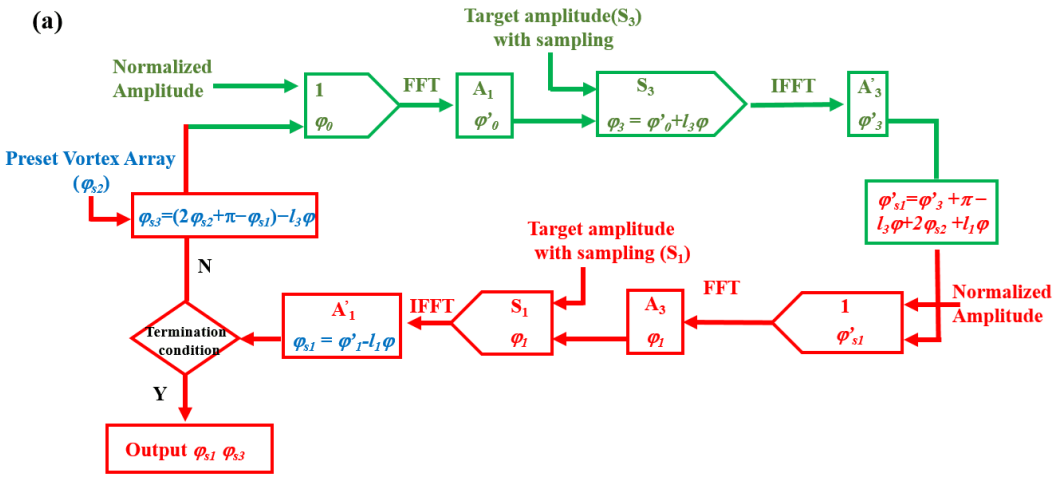

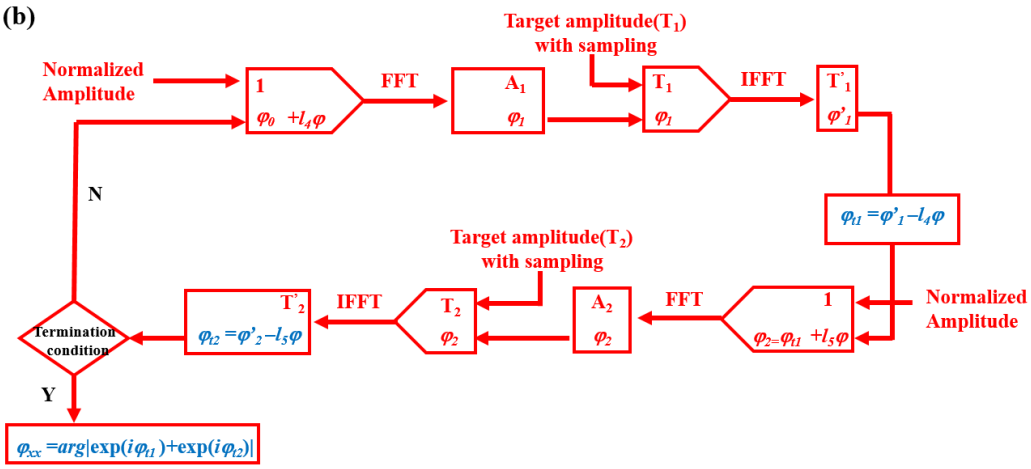

Figure S1. The flowchart of multi-channel polarization and multi-OAM hologram based on GS algorithm: (a) vortex indicator and the image erasing case algorithm; (b) mimicking STED case algorithm in T_{xx}, the same as T_{yy}. $arg|\cdot|$ means phase angle of the complex-valued matrix.

2. Numerical Simulations and Experimental Setup

The polarization selective reconstruction is based on the birefringent property of metasurface. We carry out 2D parameter optimization of nanofins using a rigorous coupled-wave analysis (RCWA) method. The height (H) and the period (P) of the silicon nanofins are fixed at 600 nm and 400 nm, respectively, and sweep the length (L) and width (W) in the range of 80–280 nm at a working wavelength of 800 nm. The phase and amplitude distribution of the transmitted light for different rectangular cross-sections are shown in **Figure S2**. Note, the phase distribution of φ_{xx} and φ_{yy} covers the full 0-2π range while achieving different phase combinations with almost uniform amplitude distributions. Subsequently, the calculated phase distributions are encoded to the nanofin arrays by using suitable parameter sets from our parameter sweep.

For the reconstruction of the metasurface holograms by an incident beam with OAM, the optical setup is built as shown in the main text (**Figure 2e**). Two linear polarizers are used to select the desired incident/transmitted linearly polarized beam before and after the sample. A spatial light modulator (SLM) is used to generate the vortex light with different topological charges. To ensure that the appropriate size of the vortex beam illuminated on the sample, we placed the 4*f* (f_1=500mm, f_2=40mm) system in front of the sample (not shown), maintaining the proper magnifying ratio. An objective lens (×60/N.A. = 0.85) is used to collect the information and image the Fourier plane.

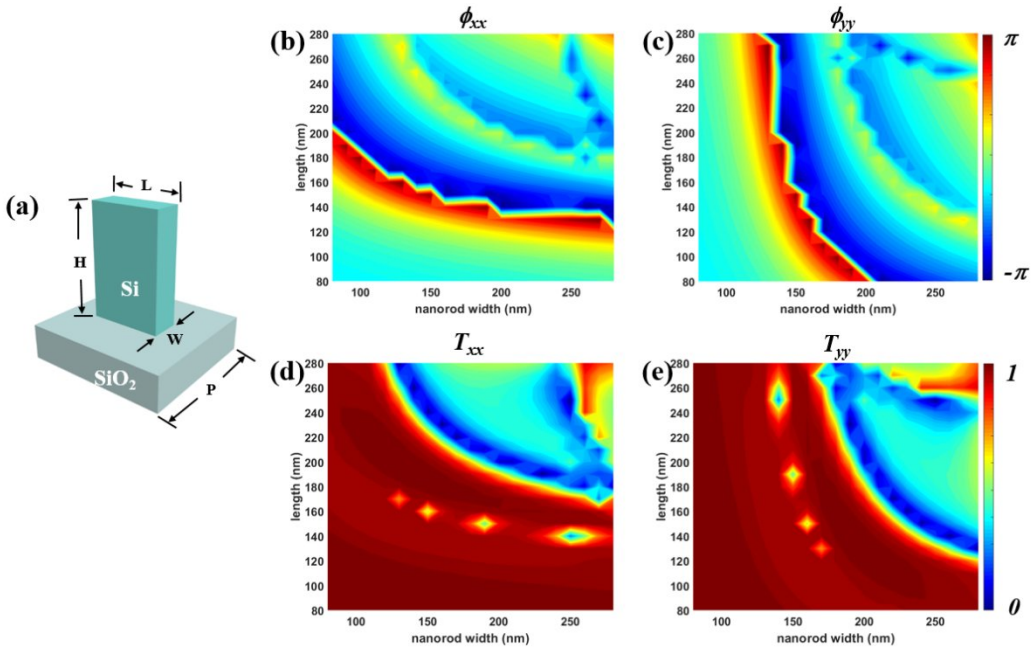

Figure S2. Simulated amplitude and phase of the transmission coefficients of the silicon nanofin. (a) Schematic illustration of an amorphous silicon nanofin positioned on a glass substrate. (b–e) Simulation results for the phase and normalized amplitude as a function of the nanofin width (w) and length (L).

3. OAM Holography in Multiple Polarization Channels

We design another sample for the demonstration of multi-polarization combination, including the linear polarization and circular polarization channels. For easier demonstration, we choose the same OAM (l=40) that is added to each polarization channel. As shown in **Figure S3**, when illuminating the x-polarized or y-polarized light carrying OAM with l=0 (plane wave), no valid information can be obtained (**Figure S3a-c**). While for the vortex beam illumination, we achieve twelve channels in total with different combinations of the flower stems and corollas. For illumination with the x-polarized light carrying OAM with l=40, the flower stem/ right flower/left flower is reconstructed in the channel T_{xx} /T_{xy} /T_{yy}, as shown in **Figure S3d-f**, respectively. Note that in experiments there is an inherent residual zero-order donut-shaped spot in the co-polarization channels of T_{xx}/T_{yy}, while for the cross-polarization channel the zero-order is negligible. When the x-polarized light is carrying OAM with l=40, one flower in the lower right corner and the stem combination (T_x) is reconstructed without output polarization selection shown in **Figure S3g**. For incident y-polarization, two flowers are detected diagonally (**Figure S3h**). While for the circular polarization illumination, all parts of the flowers are reconstructed (**Figure S3i**).

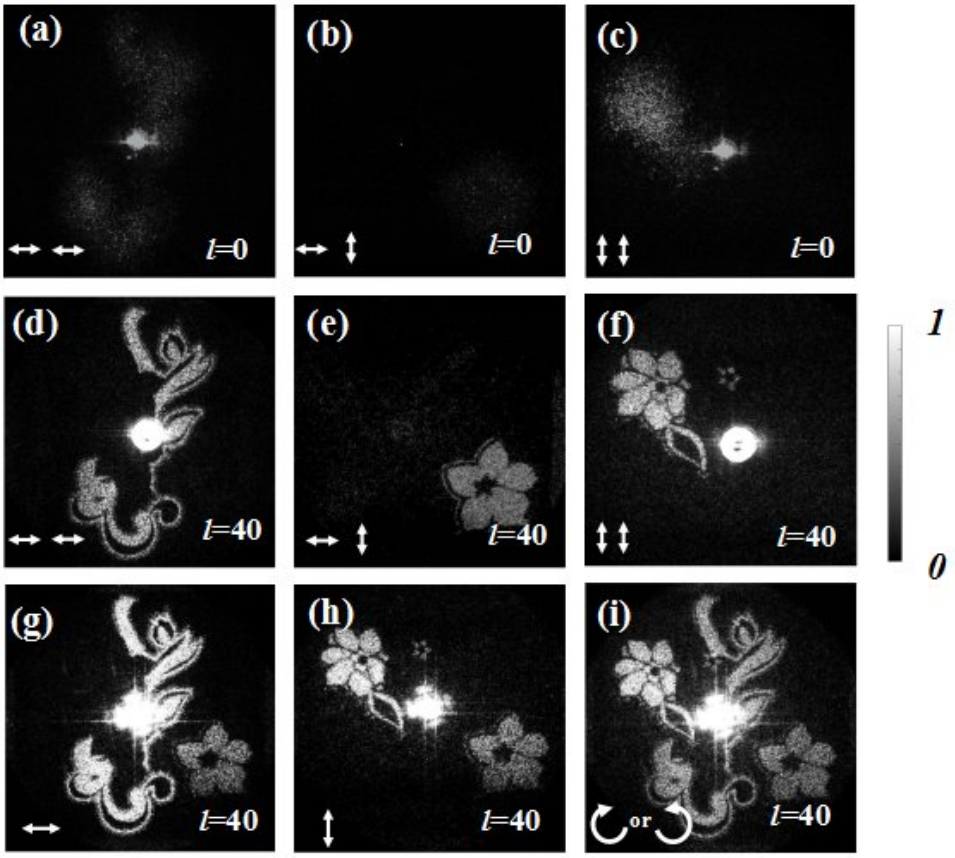

Figure S3. Experimental results of multi-polarized combination reconstruction: (a)-(c) $T_{xx}/T_{yx}/T_{yy}$ experimental result with l=0; (d)-(f) $T_{xx}/T_{yx}/T_{yy}$ experimental result with l=40; (g) (h)T_x/T_y experimental result with incident l=40 and no ouput polarized selection; (i) experimental result with circle-polarization channel and l=40; T_{yx}/T_{xy} represents x/y-polarized incident, holographic reconstruction results of y/x-polarized output. T_{yy} represents y-polarized incident, holographic reconstruction results of y-polarized output.

4. OAM Holography and Camouflage in Different Polarization Channels

We further demonstrate another case by combining the camouflage and OAM selective holography in different polarization channels to show the flexibility of the design algorithm. As shown in **Figure S4**, for an incident planar wave, no information available in the T_{xx} and T_{yy} channels (**Figure S4a,c**). While in the T_{xy} channel, a clear rose image (outside profile) is shown in the far-field (**Figure S4b**). When the incident light carries OAM with l=40, the words 'OAM' and 'BEAM' appear on the T_{xx} and T_{yy} channels (**Figure S4d,f**). While in the T_{xy} channel, a vivid rose with petals textures and leaf grooves reveals (**Figure S4e**). For a uniform comparison among different OAM incidence, we additionally incorporate experimental results with topological charge number l=10, as shown in **Figure S4g-i**, and l=20, as shown in **Figure S4j-l**. The co-polarized channels (T_{xx}, T_{yy}) become blurry. The holographic reconstruction in the cross-polarization channel shows a trend of transition from contour rose flower to rose flower with petals textures and leaf grooves. Hence, the design approach demonstrates the capabilities of a flexible and diverse design platform. By utilizing the polarization and multi-OAM modes

(different topological charges) combinations, large information capacity, high encryption security, and a variety of displays can be achieved through a single metasurface.

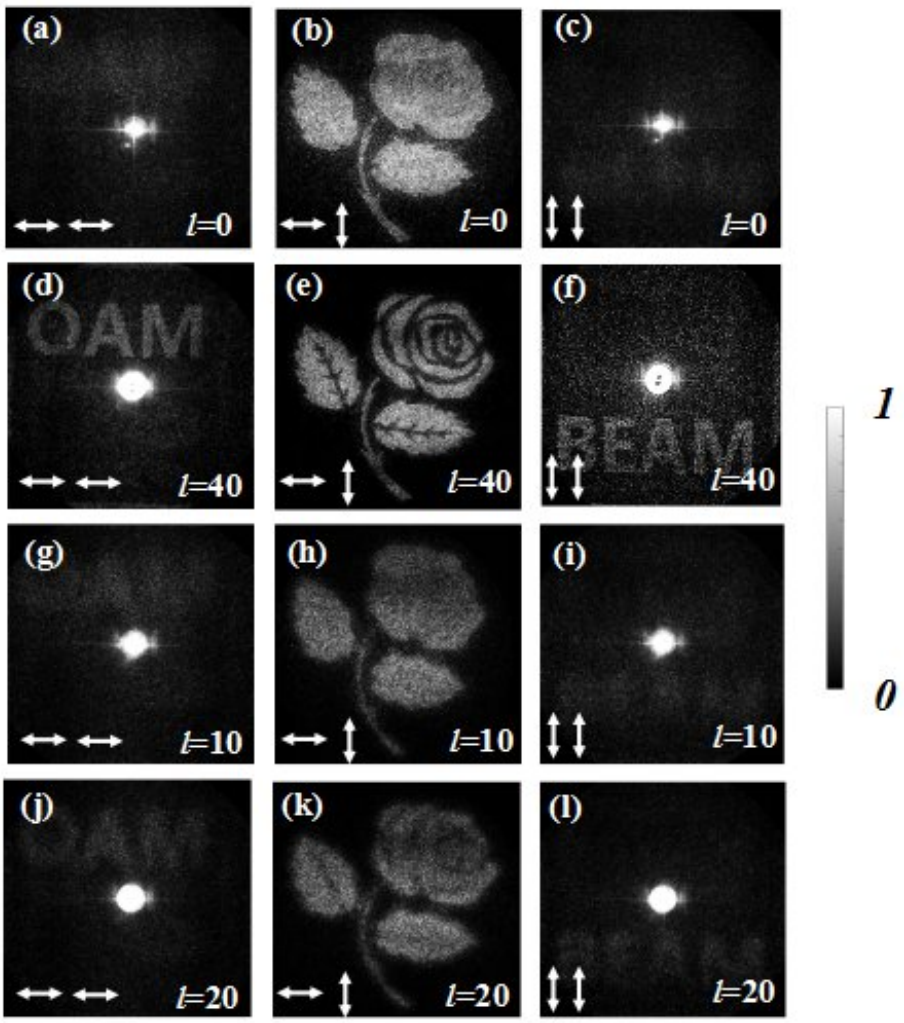

Figure S4. Experimental results of OAM holography and OAM camouflage case: (a-c) $T_{xx}/T_{xy}/T_{yy}$ experimental result with l=0. (d-f) $T_{xx}/T_{xy}/T_{yy}$ experimental result with l=40. (g-i) $T_{xx}/T_{xy}/T_{yy}$ experimental result with l=10. (j-l) $T_{xx}/T_{xy}/T_{yy}$ experimental result with l=20.

References:

1. Huang, L.; Song, X.; Reineke, B.; Li, T.; Li, X.; Liu, J.; Zhang, S.; Wang, Y.; Zentgraf, T. Volumetric Generation of Optical Vortices with Metasurfaces. *ACS Photonics* **2017**, *4*, 338-346.